Optics and Photonics Journal, 2021, 11, 441-452
https://www.scirp.org/journal/opj
ISSN Online: 2160-889X
ISSN Print: 2160-8881

Rotation Measurement Using Speckle Photography with $LiNbO_3$ Crystal: Theoretical and Experimental Analysis

Nasser A. Moustafa[1,2], H. Elgebaly[2,3]

[1]Physics Department, Faculty of Science, Helwan University, Cairo, Egypt
[2]Teachers Colleges of Makkah, Umm-Alqura University, Umm-Alqura, Saudi Arabia
[3]Physics Department, Faculty of Science, Cairo University, Giza, Egypt
Email: nasseramoustafa@gmail.com, hmelgebaly @yahoo.com

How to cite this paper: Moustafa, N.A. and Elgebaly, H. (2021) Rotation Measurement Using Speckle Photography with $LiNbO_3$ Crystal: Theoretical and Experimental Analysis. *Optics and Photonics Journal*, **11**, 441-452.
https://doi.org/10.4236/opj.2021.1110032

Received: February 9, 2020
Accepted: October 27, 2021
Published: October 30, 2021

Copyright © 2021 by author(s) and Scientific Research Publishing Inc.
This work is licensed under the Creative Commons Attribution International License (CC BY 4.0).
http://creativecommons.org/licenses/by/4.0/
Open Access

Abstract

Photorefractive crystals present varied features charming presence, such as high resolution, and normal handling. Depending on the portability of erasing images, photorefractive crystals are convenient for read-write implementations and hence find potential use in speckle photography, speckle interferometry, image processing and holography. A two-beam coupling arrangement using a $LiNbO_3$ crystal as a recording medium for real-time rotation measurement using the coherent and low-power laser source is presented in this paper. A speckle photography technique is advanced for the measurement of a small rotation of a transmitted glass slide sample. New theoretical analysis is formulated for a general case of a slide rotation. Experimental studies are carried out to verify the outcome of the theoretical predictions and accuracy of measurement. Uncertainty of rotation measurement is studied and quantified. The proposed technique is a simple, attractive and alternative method for fringe analysis. The method promises a high degree of accuracy and increased range for rotation measurement in real-time.

Keywords

Speckle Photgraphy, Photo-Refractive Materials, Two-Beam Coupling, Measurement Uncertainty, Tilt Measurement

1. Introduction

Measurement of displacement, deformation, rotation or tilt of different objects is a basic requirement in engineering problems. Considerable disturbance can be created by any object motion in the optical setup. It is sometimes necessary to have an estimate of the motion an object has undergone. Speckle photography is the most widely used technique in this regard [1]-[8].

This technique essentially consists of recording incoherent superposition of speckle patterns generated before and after deformation. The fourier transform (FT) analysis of the recorded specklegrams reveals the information of object deformation. There was a great effort to achieve the process work in real time by replacing the conventional photographic material with dynamic photorefractive materials [9] [10] [11] [12], which makes it be possible the observation of double and multiple-exposure speckle fringes in real-time.

In-plane and out-of-plane displacement components of an object motion have been measured accurately using speckle photography [13] [14] [15], or in real time using a photorefractive speckle correlator [13]. The rotational motion (axis of rotation orthogonal to the line of sight) of the glass plate sample leads to a reduction in the contrast of the given Young's fringes.

Speckle photography studies are made using a simple two-beam coupling configuration. In speckle photography, a diffused object illuminated with the transmitted laser beam coming from the glass plate is imaged inside the crystal, and a pump beam is added at this plane. When the glass slide is rotated, the speckle patterns shift consequently. The speckle patterns due to each beam and the pump beam produce index gratings. Thus, the fields from respective points on the object interfere after passage through the crystal and produce Young's fringe patterns.

Speckle photography was first demonstrated by Tiziani *et al.* [16] for real time displacement, tilt and vibration analysis with a BSO ($Bi_{12}SiO_{20}$) crystal. An Argon Ion laser was used to create the dynamic grating of the speckle pattern inside the crystal and a low-power He-Ne laser read the grating to obtain the fringe pattern.

Nasser A. Moustafa *et al.* [17] presents an optical configuration in speckle photography to extend the applicability of the two-beam coupling configuration using $LiNbO_3$ as a recording medium for the evaluation of in-plane displacement of a transparent rough object, and measurement uncertainty of in-plane displacement was studied on a wide range of displacements using experimental and new theoretical formulae for displacement measurement.

Mohammad Tiziani *et al.* [18] present a new optical configuration in speckle shear photography to measure in-plan displacement and strain in real time using $BaTiO_3$ crystal as a recording medium. Due to starin, the fringes in each pattern are of different width and orientation, resulting in the generation of a moire pattern. The strain is obtained from the width and orientation of the fringes in the moire pattern.

The speckle photography technique is also implemented in a $BaTiO_3$ crystal [19] for real-time displacement measurement of distant objects using a high coherent source such as frequency-doubled diode-pumped Nd: YAG laser is presented. Long coherence length of the laser permits to study the objects which are far away from the $BaTiO_3$ crystal. The requirement however, is that both the objects and the recording stage should be vibration isolated, and influence of intervening medium must be negligible.

The aim of the work is to present a simple speckle technique for analysing the rotation angle by using the recorded speckle with $LiNbO_3$ as a recording medium. Uncertainty of rotation angle measurements on a wide range of displacement is given. A new mathematical formula has been discovered that confirms with high accuracy the experimental work.

2. Theoretical Background

Let us consider the transmittance of a plane wave through a transmitted glass slide of refractive index μ and thickness t surrounded by a free space.

Let $U(x,y,d)$ and $U(x,y,0)$ are the complex amplitudes of the plane wave after and before transmission respectively. Therefore the ratio $t(x,y)=U(x,y,d)/U(x,y,0)$ represent the complex amplitude transmittance of the glass slide, then

$$U(x,y,d)=a\mathrm{e}^{j\phi}\mathrm{e}^{-jkt} \tag{1}$$

where a and ϕ are the amplitude and phase of the incident wave respectively.

For measuring the rotation angle of the glass plate sample using the theory of refraction of the incident wave. The glass slide is put on a graduated rotatable disc. Spatially coherent light transmitted through the glass slide and illuminated a rough surface, as shown in **Figure 1**. The obtained speckle is recorded twice, one before the rotation, and one after the rotation of the glass slide. The two images are combined digitally, and the resultant image will contain a pair of identical speckle patterns separated by a distance $\Delta\xi$ which will be calculated experimentally.

The magnitude of the rotation angle θ can be related to the fringe spacing of the observed Young's fringes at the CCD plane, the distances between the laser source and the diffuser, and between the diffuser and the CCD plane.

The amplitude distribution after the first exposure in the observation plane is given as

$$A_1(x,y)=\iint a\mathrm{e}^{i\phi}\mathrm{e}^{-ikt}\mathrm{e}^{j\frac{\pi}{\lambda z_1}\left(\xi^2+\eta^2\right)}\mathrm{e}^{-j\frac{\pi}{\lambda z_2}\left[(x-\xi)^2+(y-\eta)^2\right]}\mathrm{d}\varsigma\mathrm{d}\eta \tag{2}$$

z_1 and z_2 are the distances between the laser source and the diffuser, and between the crystal plane and the observation plane CCD respectively.

Equation (2) can be further written as

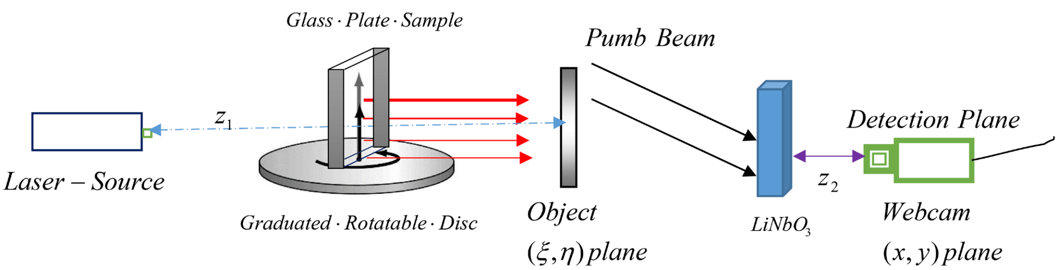

Figure 1. Basic arrangement of the speckle interference pattern recording geometry.

$$A_1(x,y) = a\mathrm{e}^{i\phi}\mathrm{e}^{-ikt}\mathrm{e}^{\frac{j\pi}{\lambda z_2}(x^2+y^2)}\iint \mathrm{e}^{\frac{j\pi}{\lambda}\left(\frac{z_1+z_2}{z_1 z_2}\right)(\xi^2+\eta^2)}\mathrm{e}^{-\frac{j2\pi}{\lambda z_2}[x\xi+\eta y]}\mathrm{d}\xi\mathrm{d}\eta \tag{3}$$

If the glass plate rotated by an angle θ with the incident wave, the angle of refraction will be θ_1. The two angles are related by the Snell's law, $\sin\theta = \mu\sin\theta_1$. In this case, the complex amplitude transmittance of the glass slide will be $\exp\left[-ik\left(t\cos\theta_1 + y\sin(\theta/\mu)\right)\right]$ [20]. Knowing that, $y\sin(\theta/\mu) \ll t\cos(\theta/\mu)$, so the complex amplitude transmittance will be $\exp\left[-ik\left(t\cos(\theta/\mu)\right)\right]$, where $\theta_1 \approx \theta/\mu$.

During the second exposure, the amplitude distribution $A_2(x,y)$ after the rotation θ of the glass slide can be expressed as

$$A_2(x,y) = \mathrm{e}^{\frac{j\pi}{\lambda z_2}(x^2+y^2)}\iint a\mathrm{e}^{i\phi}\mathrm{e}^{-ikt\cos(\theta/\mu)}\mathrm{e}^{\frac{j\pi}{\lambda}\left(\frac{z_1+z_2}{z_1 z_2}\right)\left((\xi-\Delta\xi)^2+\eta^2\right)}\mathrm{e}^{-\frac{j2\pi}{\lambda z_2}[x(\xi-\Delta\xi)+\eta y]}\mathrm{d}\xi\mathrm{d}\eta \tag{4}$$

Equation (4) can be further written as

$$\begin{aligned} A_2(x,y) = {} & a\mathrm{e}^{i\phi}\mathrm{e}^{-ikt\cos(\theta/\mu)}\mathrm{e}^{\frac{j\pi}{\lambda z_2}(x^2+y^2)}\mathrm{e}^{\frac{j\pi}{\lambda}\left(\frac{z_1+z_2}{z_1 z_2}\right)\Delta\xi^2}\mathrm{e}^{\frac{j2\pi}{\lambda z_2}x\Delta\xi} \\ & \times\iint \mathrm{e}^{\frac{j\pi}{\lambda}\left(\frac{z_1+z_2}{z_1 z_2}\right)(\xi^2+\eta^2)}\mathrm{e}^{\frac{-2j\pi}{\lambda}\left(\frac{z_1+z_2}{z_1 z_2}\right)\xi\Delta\xi}\mathrm{e}^{-\frac{j2\pi}{\lambda z_2}[x\xi+\eta y]}\mathrm{d}\xi\mathrm{d}\eta \end{aligned} \tag{5}$$

In this experiment $\Delta\xi \ll \xi$, this means that $\xi\Delta\xi \approx \text{zero}$.

So Equation (5) can be putted in the form:

$$\begin{aligned} A_2(x,y) = {} & a\mathrm{e}^{i\phi}\mathrm{e}^{-ikt\cos(\theta/\mu)}\mathrm{e}^{\frac{j\pi}{\lambda z_2}(x^2+y^2)}\mathrm{e}^{\frac{j\pi}{\lambda}\left(\frac{z_1+z_2}{z_1 z_2}\right)\Delta\xi^2}\mathrm{e}^{\frac{j2\pi}{\lambda z_2}x\Delta\xi} \\ & \times\iint \mathrm{e}^{\frac{j\pi}{\lambda}\left(\frac{z_1+z_2}{z_1 z_2}\right)(\xi^2+\eta^2)}\mathrm{e}^{-\frac{j2\pi}{\lambda z_2}[x\xi+\eta y]}\mathrm{d}\xi\mathrm{d}\eta \end{aligned} \tag{6}$$

By adding the two Equations (3) and (6)

$$\begin{aligned} & A_1(x,y) + A_2(x,y) \\ & = a\mathrm{e}^{i\phi}\mathrm{e}^{\frac{j\pi}{\lambda z_2}(x^2+y^2)}\left[\mathrm{e}^{-ikt} + \mathrm{e}^{-ikt\cos(\theta/\mu)}\mathrm{e}^{\frac{j\pi}{\lambda}\left(\frac{z_1+z_2}{z_1 z_2}\right)\Delta\xi^2}\mathrm{e}^{\frac{j2\pi}{\lambda z_2}x_{new}\Delta\xi}\right]F\{A(\xi,\eta)\} \end{aligned} \tag{7}$$

$$\begin{aligned} & A_1(x,y) + A_2(x,y) \\ & = a\mathrm{e}^{-i\phi}\mathrm{e}^{-ikt}\mathrm{e}^{\frac{j\pi}{\lambda z_2}(x^2+y^2)}\left[1 + \mathrm{e}^{ikt}\mathrm{e}^{-ikt\cos(\theta/\mu)}\mathrm{e}^{\frac{j\pi}{\lambda}\left(\frac{z_1+z_2}{z_1 z_2}\right)\Delta\xi^2}\mathrm{e}^{\frac{j2\pi}{\lambda z_2}x_{new}\Delta\xi}\right]F\{A(\xi,\eta)\} \end{aligned} \tag{8}$$

where x_{new} represent the fringe spacing which given by the new formulae [17]:

$$x_{new} = \frac{\lambda z_2}{M\xi_m} - \frac{\xi_m z_2}{2M}\left(\frac{z_1+z_2}{z_1 z_2}\right) \tag{9}$$

where M is the magnification of the imaging system.

The intensity distribution in the observation plane can be written as

$$\begin{aligned} I = {} & F^2\{A(\xi,\eta)\}\left|a\mathrm{e}^{-i\phi}\mathrm{e}^{-ikt}\mathrm{e}^{\frac{j\pi}{\lambda z_2}(x^2+y^2)}\right|^2 \\ & \times\left[2 + 2\cos\left(kt - kt\cos(\theta/\mu) + \frac{\pi}{\lambda}\left(\frac{z_1+z_2}{z_1 z_2}\right)\Delta\xi^2 + \frac{2\pi}{\lambda z_2}x_{new}\Delta\xi\right)\right] \end{aligned} \tag{10}$$

$$I = 2F^2\left\{A(\xi,\eta)\right\}\left|a\mathrm{e}^{-i\phi}\mathrm{e}^{-ikt}\mathrm{e}^{\frac{j\pi}{\lambda z_2}\left(x^2+y^2\right)}\right|^2 \times\left[1+2\cos\left(kt-kt\cos(\theta/\mu)+\frac{\pi}{\lambda}\left(\frac{z_1+z_2}{z_1 z_2}\right)\Delta\xi^2+\frac{2\pi}{\lambda z_2}x_{new}\Delta\xi\right)\right] \quad (11)$$

At maximum intensity

$$kt-kt\cos(\theta/\mu)+\frac{\pi}{\lambda}\left(\frac{z_1+z_2}{z_1 z_2}\right)\Delta\xi^2+\frac{2\pi}{\lambda z_2}x_{new}\Delta\xi = 2m\pi \quad (12)$$

Here m is an integer, it represents straight line fringes parallel to the y-axis.

$$\text{At } m=1,\quad kt-kt\cos(\theta/\mu)+\frac{\pi}{\lambda}\left(\frac{z_1+z_2}{z_1 z_2}\right)\Delta\xi^2+\frac{2\pi}{\lambda z_2}x_{new}\Delta\xi = 2\pi \quad (13)$$

Equation (13) shows an equation of the rotation angle, and it can be solved as:

$$\theta = \mu\cos^{-1}\left[1+\frac{1}{t}\left(\frac{\Delta\xi^2}{2}\left(\frac{z_1+z_2}{z_1 z_2}\right)+\frac{x_{new}\Delta\xi}{z_2}-\lambda\right)\right] \quad (14)$$

3. Experimental Results and Discussions

Figure 2 shows the experimental set-up of speckle recording in a $LiNbO_3$ crystal. This crystal is 5 mm × 5 mm × 5 mm in size. The optical configuration is implemented to study the rotation angle of a glass slide sample, which has a thickness 10^3 μm. The glass slide is illuminated with a coherent low power laser beam (λ = 670 nm, and P = 10 mW).

The spatially coherent light transmitted through the glass slide illuminates a rough surface, the laser beam spot at the diffuser plane was kept 2 cm in diameter

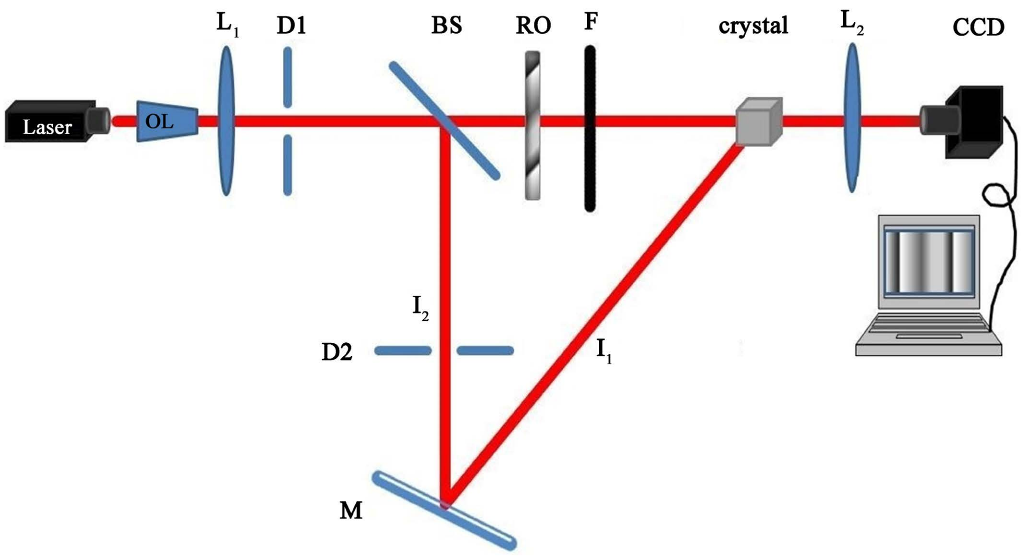

Figure 2. Experimental set-up for speckle photography with photorefractive crystal: OL: Objective lens, L_1: Lens, D1 and D2: Pupil apertures, GP: Glass palte sample, BS: Beam splitter, RO: Rough object, F: Filter, L_2: Imaging lens, Crystal $LiNbO_3$, CCD: Observation plane, M: Mirror, I_1: Average intensity of the reference plane wave, I_2: Average intensity of the pumb beam.

to ensure suitable speckle size.

Nearly half portion of the transmitted beam illuminates the diffuser. Remaining portion of the laser beam enters the crystal directly. The glass slide sample is putted on a rotatable disc. The pumb beam which given from the same laser source is adjusted at an angle 35˚ (external) with respect to the object beam. Consequently, there is an interference between the bump beam and the object beam inside the crystal creating the necessary specklegram. If a rotation given to the glass slide, the transmitted beam falls also on the object, and will result in the shift of its image at the crystal plane and this will disturb the two-beam coupling. At this instant of time in the observation plane, we have two diffracted waves, and these two waves on interference, give rise to Young's fringes at the observation plane (CCD plane). The CCD camera have a pixel resolution of 1280 × 1024, and pixel size 4.65 × 4.65 μm/pixel.

Figures 3(a)-(e) shows the Young's fringes in the spectral field, the rotation

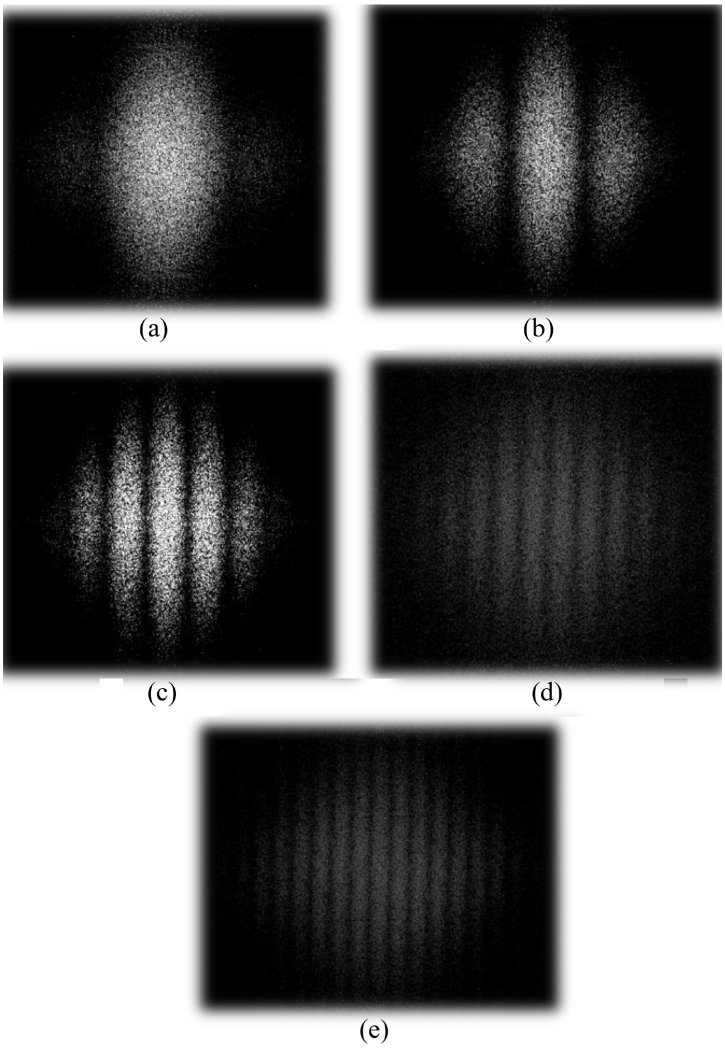

Figure 3. Images of Young's fringes in the spectral field: The rotation angle was $\theta = 0.5^{\circ}$ at wavelengths 0.4360 μm, 0.5640 μm, 0.5780 μm, 0.6328 μm, 0.6700 μm respectively. The distance between the crystal plane and the observation plane z_2 was 45 cm.

angle was $\theta = 0.5^{\circ}$ at wavelengths 0.4360 µm, 0.5640 µm, 0.5780 µm, 0.6328 µm, 0.6700 µm respectively. The distance between the crystal plane and the observation plane z_2 was 45 cm.

Figures 4(a)-(e) shows Young's fringes in the spectral field, the rotation angle of the glass sample was 1˚, 2˚, 3˚, 4˚, 5˚ respectively. The wavelength was 0.5780 µm. The distance between the crystal plane and the observation plane z_2 was 45 cm.

4. Measurement Uncertainties of Method

The uncertainty of θ was estimated by combining the standard uncertainties of the parameters $\lambda, z_1, z_2, x_{new}, \Delta\xi, d$ and μ. The relation between the value of θ and input parameters can be expressed by a model:

$$\theta = f\left(\lambda, z_1, z_2, x_{new}, \Delta\xi, d, \mu\right) \tag{15}$$

where $\lambda, z_1, z_2, x_{new}, \Delta\xi, d$ and μ represent model input parameters. The

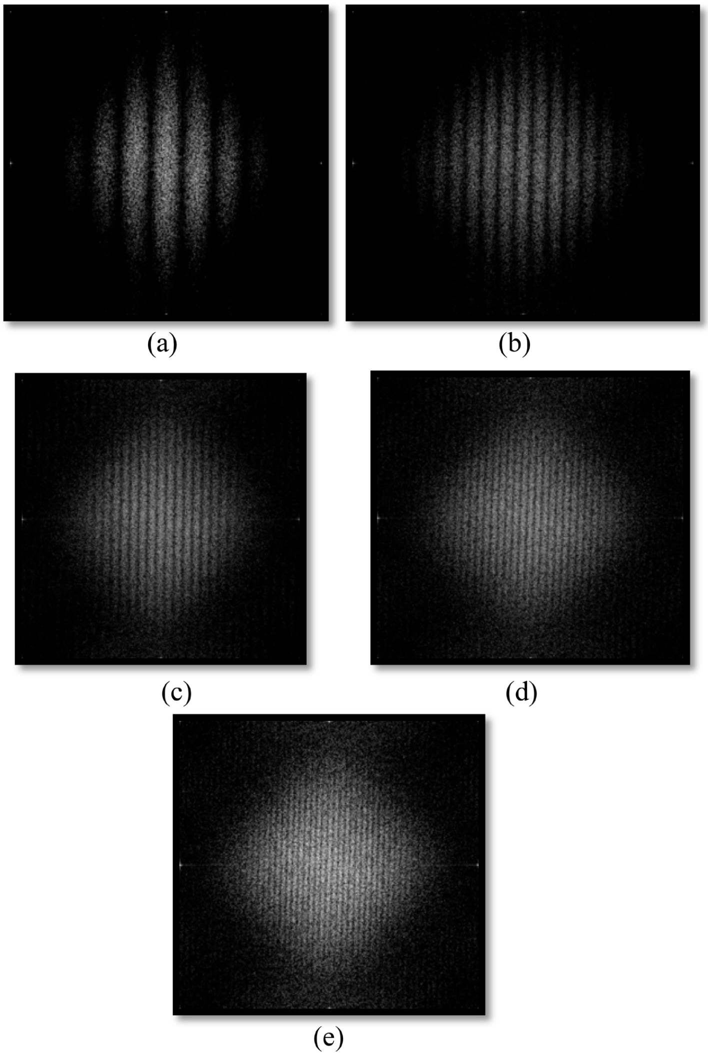

Figure 4. Show the Young's fringes in the spectral field, the rotation angle of the glass sample was 1˚, 2˚, 3˚, 4˚, 5˚ respectively. The wavelength was 0.5780 µm. The distance between the crystal plane and the observation plane z_2 was 45 cm.

uncertainty of the results $\left(u(\theta)\right)$ depends on the uncertainty of the input parameters, and can be described by the equation:

$$u(\theta)^2 = \sum_{i=1}^{N}\left(\frac{\partial\theta}{\partial y_i}\right)^2 \cdot u(y_i)^2 \tag{16}$$

where $y_1,\cdots,y_i,\cdots,y_N$ represent model input parameters, $u(y_i)\left(u(\lambda),u(z_1),u(z_2),u(x_{new}),u(\Delta\xi),u(d),u(\mu)\right)$ are the standard uncertainties of the input parameters, and $\frac{\partial\theta}{\partial y_i}$ is a sensitivity coefficient. The sensitivity coefficient describes how the measurement result varies with changes in the value of input estimates. Equation (16) is valid for measurement where there is no correlation between input parameters.

Depending on the new formulae (14) and also on the Equation (16), $\frac{\partial\theta}{\partial y_i}$ can be expressed in the form

$$\frac{\partial\theta}{\partial\lambda} = \frac{\mu}{t}\frac{1}{\sqrt{1-\left[1+\frac{1}{t}\left(\frac{\Delta\xi^2}{2}\left(\frac{z_1+z_2}{z_1 z_2}\right)+\frac{x_{new}\Delta\xi}{z_2}-\lambda\right)\right]^2}}, \tag{17}$$

$$\frac{\partial\theta}{\partial(\Delta\xi)} = \frac{-\mu}{tz_2}\frac{\left[\left(\frac{z_1+z_2}{z_1}\right)\Delta\xi + x_{new}\right]}{\sqrt{1-\left[1+\frac{1}{t}\left(\frac{\Delta\xi^2}{2}\left(\frac{z_1+z_2}{z_1 z_2}\right)+\frac{x_{new}\Delta\xi}{z_2}-\lambda\right)\right]^2}} \tag{18}$$

$$\frac{\partial\theta}{\partial(x_{new})} = -\mu\frac{\left[\frac{\Delta\xi}{tz_2}\right]}{\sqrt{1-\left[1+\frac{1}{t}\left(\frac{\Delta\xi^2}{2}\left(\frac{z_1+z_2}{z_1 z_2}\right)+\frac{x_{new}\Delta\xi}{z_2}-\lambda\right)\right]^2}} \tag{19}$$

$$\frac{\partial\theta}{\partial(t)} = -\mu\frac{\left[\frac{\Delta\xi^2}{2}\left(\frac{z_1+z_2}{z_1 z_2}\right)+\frac{\Delta\xi x_{new}}{z_2}-\lambda\right]}{\sqrt{1-\left[1+\frac{1}{t}\left(\frac{\Delta\xi^2}{2}\left(\frac{z_1+z_2}{z_1 z_2}\right)+\frac{x_{new}\Delta\xi}{z_2}-\lambda\right)\right]^2}} \tag{20}$$

$$\frac{\partial\theta}{\partial(z_1)} = \mu\frac{\left[\frac{\Delta\xi^2}{2tz_1^2}\right]}{\sqrt{1-\left[1+\frac{1}{t}\left(\frac{\Delta\xi^2}{2}\left(\frac{z_1+z_2}{z_1 z_2}\right)+\frac{x_{new}\Delta\xi}{z_2}-\lambda\right)\right]^2}} \tag{21}$$

$$\frac{\partial\theta}{\partial(z_2)} = \frac{\mu}{tz_2^2}\frac{\left[\frac{\Delta\xi^2}{2}+\Delta\xi x_{new}\right]}{\sqrt{1-\left[1+\frac{1}{t}\left(\frac{\Delta\xi^2}{2}\left(\frac{z_1+z_2}{z_1 z_2}\right)+\frac{x_{new}\Delta\xi}{z_2}-\lambda\right)\right]^2}} \tag{22}$$

and

$$\frac{\partial\theta}{\partial(\mu)} = \cos^{-1}\left[1+\frac{1}{t}\left(\frac{\Delta\xi^2}{2}\left(\frac{z_1+z_2}{z_1 z_2}\right)+\frac{x_{new}\Delta\xi}{z_2}-\lambda\right)\right] \quad (23)$$

where $\frac{\partial\theta}{\partial\lambda}$, $\frac{\partial\theta}{\partial(\Delta\xi)}$, $\frac{\partial\theta}{\partial(x_{new})}$, $\frac{\partial\theta}{\partial(t)}$, $\frac{\partial\theta}{\partial(z_1)}$, $\frac{\partial\theta}{\partial(z_2)}$ and $\frac{\partial\theta}{\partial(\mu)}$ are the sensitivity coefficient of the wavelength of the used light, the sensitivity coefficient of the distance between a pair of identical speckle patterns, the sensitivity coefficient of the fringe spacing calculated by the new formulae [20], the sensitivity coefficient of the thickness of the rotatable glass slide, the sensitivity coefficient of the distance between the laser source and the diffuser, the sensitivity coefficient of the distance between crystal plane and the observation plane CCD, and the sensitivity coefficient of the refractive index of the rotatable glass slide respectively.

Figure 5 shows the dependence of the fringe spacing of Young's fringes on the rotation angle of the glass slide sample for different wavelengths at constant values of z_1 = 65 cm and z_2 = 45 cm. From that figure, we can conclude that the experimental measurements of the rotation angle is in good agreement with the theoretical new formulae (13), for given that angle.

Image processing program, Java-based image processing program was used for the calculation of the fringe spacing of the experimental results for giving the rotation angle theoretically.

Figure 6 shows the dependence of the combined uncertainty on the rotation

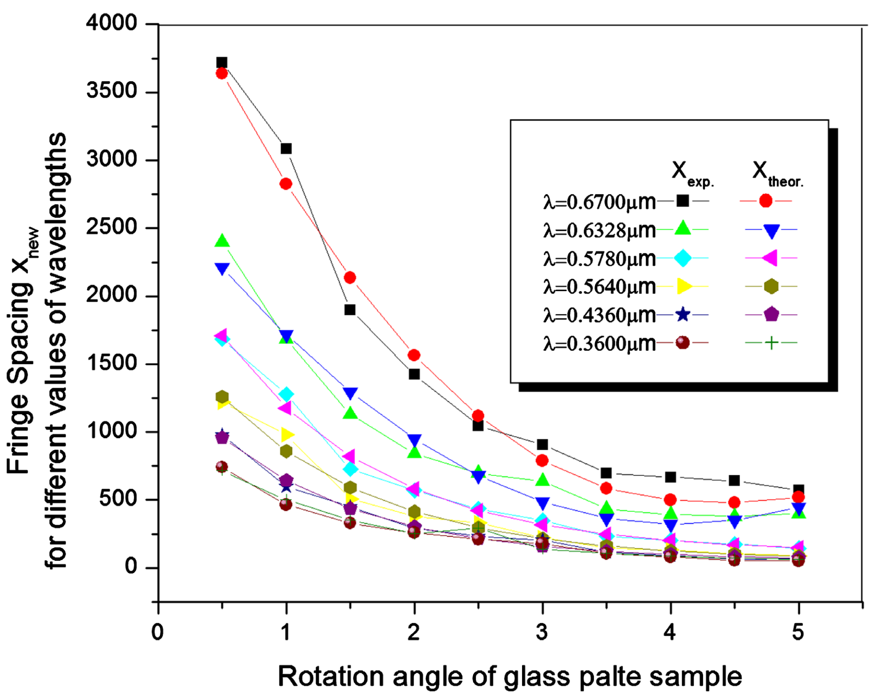

Figure 5. Dependence of the the combined uncertainty on changing the rotation angle of the glass palte sample θ for different values of wavelengths at constant values of z_1 = 65 cm and z_2 = 45 cm.

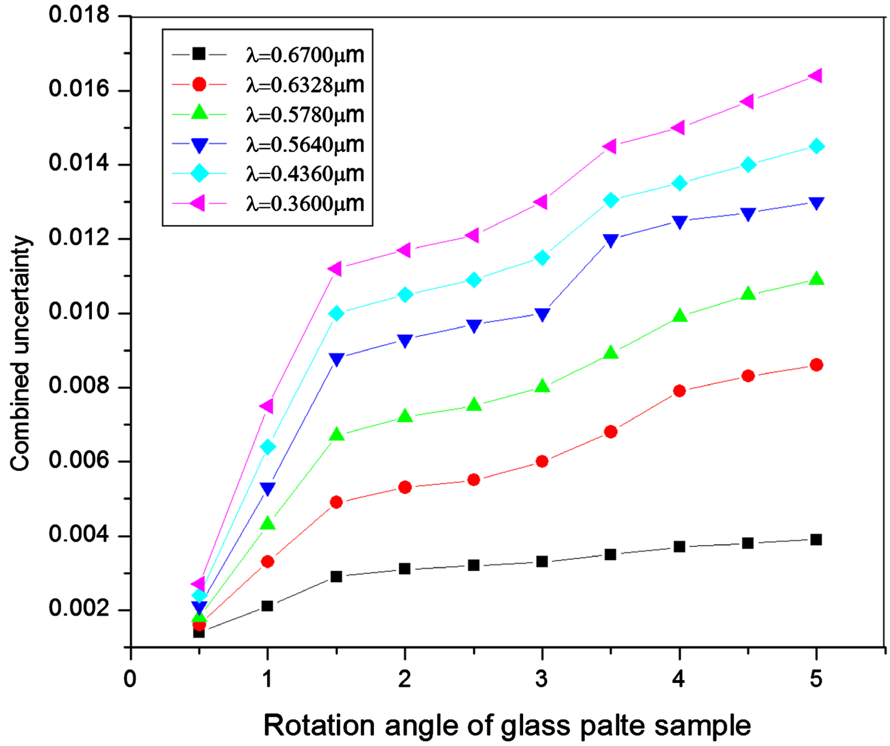

Figure 6. The relation between the fringe spacing x_{new} of Young's fringes and the rotation angle of the glass palte sample for different values of wavelengths at constant values of z_1 = 65 cm and z_2 = 45 cm.

angle of the glass slide sample at different values of wavelengths. It can be seen that at the angle 0.5˚, the values of the combined uncertainy are very close together, and getting away from each other with increasing the values of the wavelengths. The uses of laser light of wavelength 0.6700 μm give the optimum combined uncertainty for given accurate measurement of the rotation angle.

5. Conclusion

We have presented a simple speckle technique for analyzing the rotation angle by using the recorded speckle with $LiNbO_3$ as a recording medium. Uncertainty of rotation angle measurements on a wide range of changing the rotation of the glass palte sample is given. New theoretical formulae were discovered to give high documentation for the experimental work. The uses of laser light of wavelength 0.6700 μm give the optimum combined uncertainty for given accurate measurement of the rotation angle. It can be concluded that the experimental measurements of the rotation angle are in good agreement with the theoretical new formulae. This assures an increase in the efficiency of measurement, in cases where the accuracy of the measurement is of great interest.

Acknowledgements

This work is funded by grant number (12-NAN2287-10) from National Science Technology and Innovation Plan (NSTP), the King Abdul-Aziz City for Science and Technology (MAARIFH), Kingdom of Saudi Arabia. We thank the Science and Technology Unit at Umm Al-Qura University for their continuous logistic support.

Conflicts of Interest

The authors declare no conflicts of interest regarding the publication of this paper.

References

[1] Barrientos, B., Lopez, L.M., Dirckx, J.J.J. and Cywiak, M. (2004) Measurement of Out-of-Plane Deformation by Combination of Speckle Photography and Speckle Shearing Interferometry. *Optik*, **115**, 248-252. https://doi.org/10.1078/0030-4026-00362

[2] Archbold, E., Burch, J.M. and Ennos, A.E. (1970) Recording of In-Plane Surface Displacement by Double-Exposure Speckle Photography. *Optica Acta*, **17**, 883-898. https://doi.org/10.1080/713818270

[3] Stetson, K.A. (1975) A Review of Speckle Photography and Speckle Interferometry. *Optical Engineering*, **14**, 482-489. https://doi.org/10.1117/12.7971814

[4] Sjodahl, M. and Benkert, L.R. (1993) Electronic Speckle Photography: Analysis of an Algorithm Giving the Displacement with Sub Pixel Accuracy. *Applied Optics*, **32**, 2278-2284. https://doi.org/10.1364/AO.32.002278

[5] Sjodahl, M. (1994) Electronic Speckle Photography: Increase Accuracy by Non Integral Pixel Shifting. *Applied Optics*, **33**, 6667-6673. https://doi.org/10.1364/AO.33.006667

[6] Moustafa, N.A. (2009) Fourier Transform in Speckle Photography for Measuring the Refractive Index for a Transparent Plate. *Material Science Research India*, **6**, 99-104.

[7] Moustafa, N.A., El-Nicklawy, M.M., Hassan, A.F. and Ibrahim, A.K. (2013) Effect of Partially Coherent Light on the Contrast of Speckle Patterns Obtained Using Digital Image Processing of Speckle Photography. *Optics and Photonics Journal*, **3**, 324-329. https://doi.org/10.4236/opj.2013.35050

[8] Andersson, A., Mohan, N.K., Sjödahl, M. and Molin, N.-E. (2000) TV Shearography: Quantitative Measurement of Shear-Magnitude Fields by Use of Digital Speckle Photography. *Applied Optics*, **39**, 2565-2568. https://doi.org/10.1364/AO.39.002565

[9] Tiziani, H.J., Leonhardt, K. and Klenk, J. (1980) Real-Time Displacement and Tilt Analysis by a Speckle Technique Using $Bi_{12}SiO_{20}$ Crystals. *Optics Communications*, **34**, 327-331. https://doi.org/10.1016/0030-4018(80)90388-0

[10] Kamara, K., Kumar, A. and Singh, K. (1996) Out-of-Plane Displacement Measurement Using Multiple-Exposure Speckle Recording in $BaTiO_3$ Crystal: Use of Converging Beam Illumination in Free Space Geometry. *Optik*, **104**, 9-14.

[11] Kamara, K., Kumar, A. and Singh, K. (1996) In-Plane-Displacement Measurement Using Objective Speckles in Photorefractive Two-Beam Coupling Effect of Multiple Exposures. *Optics Communications*, **126**, 135-142. https://doi.org/10.1016/0030-4018(96)00024-7

[12] Tripathi, R., Pati, G.S., Kumar, A. and Singh, K. (1998) Object Tilt Measurement Using a Photorefractive Speckle Correlator: Theoretical and Experimental Analysis.

Optical Engineering, **37**, 2979-2987. https://doi.org/10.1117/1.601887

[13] Tripathi, R., Pati, G.S., Kumar, A. and Singh, K. (1998) In-Plane Displacement Using a Photorefractive Speckle Correlator. *Optics Communications*, **149**, 355-365. https://doi.org/10.1016/S0030-4018(98)00016-9

[14] Kumar, A. and Singh, K. (1990) Speckle Photography of Out-of-Plane Motion: Effect of Multiple-Exposures in Free Space Geometry of Recording. *Journal of Optics* (*Paris*), **21**, 19-25. https://doi.org/10.1088/0150-536X/21/1/003

[15] Majles Ara, M.H. and Sirohi, R.S. (2007) Speckle Interferometry Methods for Displacement and Strain Measurements Using Photorefractive Crystal. *Optik*, **118**, 445-451. https://doi.org/10.1016/j.ijleo.2006.04.012

[16] Tiziani, H.J., Leonhardt, K. and Klenk, J. (1980) Real-Time Displacement and Tilt Analysis by a Speckle Technique Using $Bi_{12}SiO_{20}$. *Optical Communication*, **34**, 327. https://doi.org/10.1016/0030-4018(80)90388-0

[17] Moustafa, N.A. (2020) Measurement Uncertainty of In-Plane Displacement Field Distribution Using Speckle Photography with $LiNbO_3$ Crystal. *Optical Engineering*, **59**, Article ID: 024108. https://doi.org/10.1117/1.OE.59.2.024108

[18] Majles Ara, M.H., Vijayan, C.V., Krishna Mohan, N.K. and Sirohi, R.S. (1999) Real-Time Speckle Shear Photography Using $BaTiO_3$ for In-Plane Strain and Displacement Measurements at Multiple Wavelengths. *Proceedings SPIE* 3801, *Photorefractive Fiber and Crystal Devices*: *Materials*, *Optical Properties*, *and Applications V*, Denver, 18-19 July 1999. https://doi.org/10.1117/12.363934

[19] Mohana, N.K., Darlina, J.S., Majles Araa, M.H., Kothiyala, M.P. and Sirohia, R.S. (1998) Speckle Photography with $BaTiO_3$ Crystal for the Measurement of In-Plane Displacement Field Distribution of Distant Objects. *Optics and Lasers in Engineering*, **29**, 211-216. https://doi.org/10.1016/S0143-8166(97)00086-9

[20] Saleh, B.E.A. and Teich, M.C. (1990) Fundamental of Photonics. Wiley, Hoboken, 55-56.